

**Comparison of observed and modeled drifter trajectories in
coastal regions: an improvement through adjustments for
observed drifter slip and errors in wind fields**

K.P. EDWARDS¹, F.E. WERNER¹, AND B.O. BLANTON¹

¹*Department of Marine Sciences, University of North Carolina - Chapel Hill*

Submitted, *Journal of Atmospheric and Oceanic Technology*, May 26, 2005

March 21, 2006

Corresponding author address:

K.P. Edwards, Department of Marine Sciences 12-7 Venable Hall CB 3300 UNC-CH Chapel Hill,
NC 27599

E-mail: kpehrson@email.unc.edu

ABSTRACT

Lagrangian particle tracking using three-dimensional (3-D) numerical modelling approaches has become an important tool in coastal oceanography. In this note, we describe an approach that can reduce the difference between observed and numerical drifter trajectories in the coastal ocean by including corrections to the water velocity due to differences between observed winds and the wind field used to drive the 3-D circulation model and some specific characteristics of the observed drifters in the algorithm that estimates the numerical trajectory. Quantitative improvements are obtained whereby the separation distance between the numerical and observed drifters is almost halved (in our particular field case from 2.6 km d^{-1} to 1.4 km d^{-1}).

1. Introduction

Three-dimensional (3-D) numerical modeling incorporating Lagrangian methods (e.g. particle tracking) has become an important tool in coastal oceanography (Mariano et al. 2002). Lagrangian data bring additional insight to circulation fields by providing direct observations of water parcel (or drifter) movement and transport pathways. Typically, comparisons between observed and modeled trajectories are of short duration, with separation distances between observed and modeled trajectories of several kilometers per day (Werner et al. 1999; Lynch et al. 2001).

However, Lagrangian description of flows over several weeks may be required to assess larval transport (Hare et al. 1999; Epifanio and Garvine 2001; Werner et al. 2000), pollutant dispersal (Spaulding et al. 1994), oil spill containment (Reed et al. 1997; Aamo et al. 1997; Daniel et al. 2003a), and other applications. In these cases, separation distances between predicted and observed values on the order of 100 km may result. These separations may be unacceptably large if, for example, the larval transport is being used to define marine protected areas. Some of the differences are due to missing flow components, sub-gridscale motions (i.e., frontal instabilities, response to sea breezes, etc.) in the modeled ocean circulation, incomplete knowledge of the wind field and unrealistic treatment of the drifter properties (i.e., drag characteristics). Enhancements to particle tracking algorithms for specific applications include the modeling of oil characteristics and behavior (Reed et al. 1997; Aamo et al. 1997), the addition of large-scale currents and a wave model in oil spill predictions (Daniel et al. 2003b), and the inclusion of cargo container drag characteristics (Daniel et al. 2002).

Our objective is to quantify the sources of error in our numerical particle trajectories and to provide a possible method to improve the numerical trajectories relative to the observed drifters.

In this note, we describe an approach that can reduce the difference between observed and modeled drifter trajectories in the coastal ocean by including corrections to the wind field and the drifters' slip characteristics in the algorithm that estimates the modeled trajectory. Quantitative improvements are obtained whereby the separation distance is almost halved (in our particular field case from 2.6 km d^{-1} to 1.4 km d^{-1}).

2. Lagrangian Tracking Model

Model drifters were tracked hourly using a time-stepping version of the particle tracking algorithm described by Blanton (1993) for 3-D drogue tracking on a finite element grid with linear finite elements. A fourth order Runge-Kutta scheme is used to integrate over a specified time interval and provide the ending drogue location in each time step. This scheme assumes that the particles being tracked are massless, passive particles in the 3-D flow field. The adjustments are provided in three separate steps: the first adjusts for the differences between the wind stress used to drive the 3-D circulation model and local observations, and the second adjusts the model drifter trajectories for observed slippage. Finally, the linear combination of both observed slippage and wind stress differences are calculated.

a. Correction due to differences between modeled and observed wind-stress

When the domain being considered is large, the spatial structure of the wind field (e.g., the wind stress curl) is important and can have a significant effect on currents. In this case, or when forecasts are attempted, modeled wind fields are generally used to drive ocean circulation models. While model wind fields have become quite accurate, there are differences between these model

fields and the observations. The first adjustment in the particle tracking algorithm was made to account for the difference between the model wind stress used to force the 3-D circulation model and the observed wind stress on the shelf. Welander (1957) showed that the velocity profile and flow at a given location can be expressed in terms of both the local wind-stress and the sea surface slope. Model winds, obtained from the National Centers for Environmental Prediction (NCEP) Eta Data Assimilation System (EDAS), provide both the local wind-stress and the large-scale spatial structure needed to calculate the surface slope. While there will be differences between both local measurements and the spatial structure over the large domain, we are only making corrections to the *local* wind forcing. To adjust the local wind stress, the EDAS and observed winds are compared at a single location in the domain, that being the location of the wind gauge. Thus, we assume that the difference in local measurement is roughly the same between the drifter location and the buoy where the observed winds are measured. We then use the Ekman transport relationships (e.g., Csanady 1982) and the wind stress difference at this location to adjust the model velocities:

$$u_{Ekman} = \frac{\sqrt{2}}{\rho f d} e^{\frac{z}{d}} \left[\Delta\tau_x \cos\left(\frac{z}{d} - \frac{\pi}{4}\right) - \Delta\tau_y \sin\left(\frac{z}{d} - \frac{\pi}{4}\right) \right] \quad (1)$$

$$v_{Ekman} = \frac{\sqrt{2}}{\rho f d} e^{\frac{z}{d}} \left[\Delta\tau_x \sin\left(\frac{z}{d} - \frac{\pi}{4}\right) + \Delta\tau_y \cos\left(\frac{z}{d} - \frac{\pi}{4}\right) \right] \quad (2)$$

where: $d =$ Ekman depth $\cong 0.4 \frac{u_*}{f}$

$$u_* = \text{friction velocity} = \sqrt{\frac{\tau}{\rho}}$$

$$f = \text{Coriolis parameter}$$

$$\Delta\tau_x \text{ and } \Delta\tau_y = x \text{ and } y \text{ components of wind stress difference}$$

$$\tau = \text{the observed wind stress, used to calculate } d$$

In the cases considered here, the velocity difference due to wind stress difference (u_{Ekman} and v_{Ekman}) was calculated at both the drifter depth ($z=-10$) and at the surface ($z=0$), for use in the slippage adjustment in Section 2b, and added to the model velocities at those depths.

b. Correction due to drifter slippage

Another source of error between the model and observed drifters comes from the drifters themselves. While the drifters are designed to track water parcels at the drogue depth, they do not provide a true description of the circulation. Drifters slip from true motion due to several factors, including: drag on both the tether and drogue induced by shear currents, wind drag on the surface float, and wave rectification (Geyer 1989). In the same paper, Geyer (1989) estimates slip velocities based on field experiments from 1.2 cm s^{-1} to 2.3 cm s^{-1} (approximately 1.0 to 2.0 km day^{-1}) for holey sock drogues with 20 cm (8 inch) spherical floats.

To incorporate a slippage-velocity into the particle tracking algorithm, we use Geyer's (1989) derived relationship between surface velocity and drifter slip velocity due to drag on the surface float caused by velocity shear in the water column:

$$U_s = U_{surface} \sqrt{\frac{C_f}{C_d}} \sqrt{\frac{A_f}{A_d}} \quad (3)$$

where $U_{surface}$ = the model surface velocity, $(C_f, C_d) = (0.5, 1.0)$ are dimensionless constants reflecting the drag coefficient on the float and drogue, respectively, and $[A_f, A_d \text{ (m}^2\text{)}]$ are drogue-specific values of the float and drogue and are calculated from the drifter dimensions provided in Section 3c. By relating the magnitude of U_s to the other sources of slip provided in Geyer (1989), an estimate of the total slip velocity for the observed drifters is given by:

$$U_{slip} = 2.75 U_s \quad (4)$$

c. Combined Correction

The total velocity acting on the numerical drifters is then given by:

$$U_{drifter} = U_{10m} + U_{Ekman} + U_{slip} \quad (5)$$

where: U_{10m} = model velocity at 10m

3. Case Study

A field-scale evaluation of this formulation was implemented in the Southeast U.S. Continental Shelf (SEUSCS) with observed winds which were obtained from the National Data Buoy Center (NDBC) buoy located within the Grays Reef National Marine Sanctuary (GRNMS) (Figure 1) and observed drifters released in GRNMS in October 2000. The observed wind stress was computed from the wind speed as described in Large and Pond (1981); Blanton et al. (1987).

a. Circulation Model

The circulation model, described in Lynch and Werner (1991) and Lynch et al. (1996) is a free-surface 3-D finite element time-stepping model of the shallow-water equations with conventional Boussinesq and hydrostatic assumptions. The model domain extends from south of Cape Canaveral, FL to Cape Fear, NC (Figure 1). The model grid has 21 vertical levels and uses terrain-following vertical coordinates configured to resolve both surface and bottom boundary layers. Horizontal grid spacing is variable with the smallest grid spacing of order 1 km near the coast and is run with a minimum bathymetric depth of 2 m.

FIG. 1

The circulation model was forced by both wind stress and tides. The wind field was obtained

from the National Centers for Environmental Prediction (NCEP) Eta Data Assimilation System (EDAS). The EDAS atmospheric forcing fields used herein are provided at 32 km resolution and at 3 h intervals. The 10 m winds are interpolated onto the SEUSCS grid, and are converted to wind stress using Large and Pond (1981). Tidal boundary conditions for M_2 , N_2 , S_2 , O_1 , K_1 , are included as described in Blanton et al. (2004), also included are K_2 , Q_1 and P_1 . Full 3-D model output is provided every hour which is used to compute the Lagrangian trajectories.

b. Differences between EDAS and observed winds

The differences in the east-west (u) and north-south (v) wind stress at the GRNMS buoy are shown in Figures 2 (a and b). During non-storm periods, the EDAS winds generally compare favorably with the observed winds. However, during the storm event around 10 October, the maximum difference between the EDAS and observed winds is greater than 0.15 Pa in the north-south direction (τ_y) and is almost 0.10 Pa in the east-west direction ($\Delta\tau_x$). While the storm event around 24 October had smaller winds, the maximum difference in $\Delta\tau_y$ is the same as earlier and for a longer time period.

FIG. 2

c. Lagrangian Data

In October 2000, three ARGOS drifters were released in the SEUSC in the vicinity of GRNMS off the coast of Georgia (see Figure 1). Table 1 provides the drifter number, time and position of first recording for each of the drifters used in this comparison. The table also provides the total number of days the observed drifters were tracked on the SEUSCS. The drifters were WOCE SVP holey sock drifters drogued at a depth of 10 m. The drogues were 6 m long and 1 m in diameter

with spherical floats either 34 cm (13.5 inches) or 40.6 cm (16 inches) in diameter. Due to the size and depth of the drogues, any drifters moving into water shallower than 15 m are assumed to drag the bottom. The data used here are the error-checked raw data as reported by ARGOS (not interpolated to regular time intervals) with an estimated error of < 1000 m. The particles are tracked in the 3D flow fields computed in Edwards et al. (accepted) with starting times and locations corresponding to the first satellite record from the observed drifters. The trajectories were integrated for approximately one month, and the model drifters were kept at 10 m depth to match the mid-depth of the drogues released in the field. Model trajectories were then sampled at the reporting times of the observed drifters for analysis and display purposes.

Although there are other drifter deployments described in Edwards et al. (accepted), we have chosen to use the October deployment because it had one of the worst comparisons between observed and modeled drifters in the unadjusted particle tracking implementation and the highest root mean square (rms) error between the EDAS and observed winds at GRNMS in the along-shelf direction (Edwards et al. accepted).

Table 1

The velocity adjustments, U_{Ekman} and U_{slip} are shown in Figure 2 c and d. The U_{slip} adjustments are generally larger; the U_{Ekman} adjustments track the wind-stress differences shown in Figure 2 a and b. Velocity measurements are calculated from the drifter position data, interpolated to 3 hr intervals, for all of the observed and numerical drifters. Figure 3 provides the drifter velocities low-pass filtered to remove the tidal signal. The mean velocities are included in Table 2.

FIG. 3

4. Discussion and Summary

Table 2 and Figures 4 and 5 present the model results including a comparison of one of the

observed drifter paths with the numerical drifter paths (Figure 4, Drifter #30351). The separation of the drogues over the integration time ranges from 77 km in the unadjusted model to 45 km after 31 days with both corrections. A linear regression (Table 2 and Figure 5) shows an improvement in the drifter separation rate with a slope of 2.6 km d^{-1} in the unadjusted model to only 1.4 km d^{-1} in the particle tracks adjusted for both wind and slip. A comparison of the separation rates between the numerical and observed drifters for all fifteen drifters released in 2000 and 2001 at GRNMS, shows a separation rate of 2.6 km d^{-1} for the unadjusted model versus 2.0 km d^{-1} .

In each case, the corrected numerical drifter trajectories provide better agreement with the observed drifters. Figure 2 provides a comparison of the model velocity adjustments with the difference in wind stress. Maximum adjustments due to the difference between EDAS and observed wind stress (U_{Ekman}) are approximately 4.5 cm s^{-1} in the north-south (v) direction while the maximum adjustments for the drifter slippage (U_{slip}) are approximately 9 cm s^{-1} during the large wind events around 10 October and 24 October providing an increase in velocity generally in the same direction as the wind stress. This adjustment is considerably larger than that estimated by Geyer (1989) and may be due to several factors including: the use of a larger surface buoy (34 cm and 40.6 cm versus 20 cm), deeper deployment of the drogues (10 m versus 5 m), and a different tidal regime, wave field and water column shear. Mean velocity adjustments (U_{Ekman} and U_{slip}) are also southward on the order of 0.2 cm s^{-1} and 0.9 cm s^{-1} for the wind stress and drifter slippage adjustments, respectively.

During the first few days of drifter deployment, there is very little separation between the observed and numerical drifters for all experiments. However, during the storm event on 10 October, the models diverge from the observed drifters. In order to explore the effect of the 10 October wind event on post-storm drifter trajectories, we reinitialized the comparison to begin after the

storm and compared the resulting drifter separation over the remaining time (not shown). We did not obtain a significant improvement in separation rates. A linear regression still shows improvement with the adjustments to the particle tracking algorithm. The unadjusted model does slightly better with a drifter separation rate of 2.2 km d^{-1} while the numerical drifters adjusted for both wind and slip have a separation rate of 1.7 km d^{-1} .

Table 2

The methods presented herein provide a simple adjustment for differences in model wind forcing and observed drifter slippage for holey-sock drogues. It also allows an improved comparison between model and observed drifter trajectories and provides a useful tool for model validation. This method probably works best in coastal regions where the forcing and response are relatively deterministic such as where tidal and wind forcings are dominant, with open ocean situations chaotic (eddy) motions present a different set of challenges. Further model validation, additional drifter release dates, and comparison to Eulerian data can be found in Edwards et al. (accepted). In that year-long Lagrangian study of circulation on the Southeast U.S. continental shelf, we find that the observed versus model drifter separation distances using the methods described here are less than 2 km d^{-1} .

FIG. 4

FIG. 5

Acknowledgements. The authors thank Jon Hare of the NOAA NMFS NEFSC Narragansett Laboratory, RI for the observed drifter data. We thank the reviewers for providing comments that greatly improved earlier versions of the manuscript. Funding from SEACOOS and a contract from the Center for Coastal Fisheries and Habitat Research to the University of North Carolina - Chapel Hill from funds provided by the Office of National Marine Sanctuaries (NOAA NOS) in support of research at Gray's Reef National Marine Sanctuary is gratefully acknowledged.

REFERENCES

- Aamo, O. M., M. Reed, and A. Lewis, 1997: Regional Contingency Planning Using the OSCAR Oil Spill Contingency and Response Model. *Proceedings of the 1997 Oil Spill Conference*.
- Blanton, B. O., 1993: User's Manual for 3-Dimensional drogue tracking on a finite element grid with linear finite elements. Technical report, UNC Marine Science, Chapel Hill, NC.
- Blanton, B. O., F. E. Werner, H. Seim, R. A. Luettich, Jr., D. R. Lynch, K. W. Smith, G. Voulgaris, F. M. Bingham, and F. Way, 2004: Barotropic tides in the South Atlantic Bight. *J. Geophys. Res.*, **109**, doi:10.1029/2004JC002455.
- Blanton, J. O., T. N. Lee, L. P. Atkinson, J. M. Bane, A. J. Riordan, and S. SethuRaman, 1987: Oceanographic studies during GALE. *Trans. Am. Geophys. Union (EOS)*, **68**, 1626–27, 1636–37.
- Csanady, G. T., 1982: *Circulation in the Coastal Ocean*. D. Reidel Publishing Company, Dordrecht, Holland.
- Daniel, P., G. Jan, F. Cabioch, Y. Landau, and E. Loiseau, 2002: Drift modeling of cargo containers. *Spill Science and Technology Bulletin*, **7**, 279–288.
- Daniel, P., P. Josse, P. Dandin, J.-M. Lefecre, G. Lery, F. Cabioch, and V. Gouriou, 2003a: Forecasting the Prestige oil spills. *Proceedings of the Interspill 2004 conference*, Trondheim, Norway.
- Daniel, P., F. Marty, P. Josse, C. Skandrani, and R. Benshila, 2003b: Improvement of drift calculation in MOTHY operational oil spill prediction system. *Proceedings of the 2003 International Oil Spill Conference*, American Petroleum Institute, Washington, D.C.
- Edwards, K. P., J. A. Hare, F. E. Werner, and B. O. Blanton, accepted: Lagrangian Circulation on

- the Southeast U.S. Continental Shelf: implications to larval dispersal and retention. *Continental Shelf Research*.
- Epifanio, C. E. and R. W. Garvine, 2001: Larval Transport on the Atlantic Continental Shelf of North America: a Review. *Estuarine, Coastal and Shelf Science*, **52**, 51–77.
- Geyer, W. R., 1989: Field calibration of mixed layer drifters. *Journal of Atmospheric and Oceanic Technology*, **6**, 333–342.
- Hare, J. A., J. A. Quinlan, F. E. Werner, B. O. Blanton, J. J. Govoni, R. B. Forward, L. R. Settle, and D. E. Hoss, 1999: Larval transport during winter in the SABRE study area: results of a coupled vertical larval behaviour-three-dimensional circulation model. *Fisheries Oceanography*, **8**, 57–76.
- Large, W. G. and S. Pond, 1981: Open ocean momentum flux measurements in moderate to strong winds. *J. of Phys. Oceanogr.*, **11**, 324–336.
- Lynch, D. R., J. T. C. Ip, C. E. Naimie, and F. E. Werner, 1996: Comprehensive coastal circulation model with application to the Gulf of Maine. *Cont. Shelf Res.*, **16**, 875–906.
- Lynch, D. R., C. E. Naimie, J. T. Ip, C. V. Lewis, F. E. Werner, R. A. Luettich, B. O. Blanton, J. A. Quinlan, D. J. McGillicuddy, J. R. Ledwell, J. Churchill, V. Kosnyrev, C. S. Davis, S. M. Gallagher, C. J. Ashjian, R. G. Lough, J. Manning, C. N. Flagg, C. G. Hannah, and R. C. Gorman, 2001: Real-time data assimilative modeling on Georges Bank. *Oceanography*, **14**, 65–77.
- Lynch, D. R. and F. E. Werner, 1991: Three-dimensional hydrodynamics on finite elements. Part II: Non-linear time-stepping model. *Int. J. Numer. Methods Fluids*, **12**, 507–533.
- Mariano, A. J., A. Griffa, T. M. Özgökmen, and E. Zambianchi, 2002: Lagrangian Analysis and Predictability of Coastal and Ocean Dynamics 2000. *Journal of Atmospheric and Oceanic*

Technology, **19**, 1114–1126.

Reed, M., O. M. Aamo, and R. S. Daling, 1997: OSCAR: a tool for strategic analysis of oil spill response analysis. *Water for a changing global community: the 27th Congress of the International Association for Hydraulic Research*, San Francisco, California.

Spaulding, M. L., V. S. Kolluru, E. Anderson, and E. Howlett, 1994: Application of Three-Dimensional Oil Spill Model (WOSM/OILMAP) to Hindcast the *braer* spill. *Spill Science & Technology Bulletin*, **1**, 23–35.

Welander, P., 1957: Wind action on a shallow sea: some generalizations of Ekman's theory. *Tellus*, **9**, 45–52.

Werner, F. E., B. O. Blanton, J. A. Quinlan, and J. R. A. Luetlich, 1999: Physical oceanography of the North Carolina continental shelf during the fall and winter seasons: implications for the transport of larval menhaden. *Fisheries Oceanography*, **8**, 7–21.

Werner, F. E., B. R. Mackenzie, R. I. Perry, R. G. Lough, C. E. Naimie, B. O. Blanton, and J. A. Quinlan, 2000: Larval trophodynamics, turbulence and drift on Georges Bank: A sensitivity analysis of cod and haddock. *Scientia Marina*, **65**, 99–115.

K.P. Edwards et al.

Generated with ametsocjmk.cls.

Written by J. M. Klymak

mailto:jklymak@coas.oregonstate.edu

http://pender.coas.oregonstate.edu/WorkTools.html

Tables

Table 1. First reported drifter time and location for the 3 drifters released near Gray's Reef National Marine Sanctuary in October 2000. The last column is the number of days which the observed drifters were tracked on the SEUSCS.

Drifter	Release Time	Latitude	Longitude	Days Tracked
30351	Oct 3, 2000 21:07	-80.859	31.372	59.62
30372	Oct 3, 2000 20:58	-80.871	31.388	59.69
30374	Oct 3, 2000 20:48	-80.884	31.373	23.12

Table 2. Results of particle trajectory corrections including: the average net displacement of the drifters (km); the mean east-west (u) and north-south (v) velocities (m s^{-1}), the average ending separation distance between the observed and modeled trajectories (km); a linear regression analysis of the average separation rate (km d^{-1}) and its r^2 value.

Model	Net displ. (km)	Mean velocity (m s^{-1})		Ending Sep. (km)	Avg. Sep. Rate (km d^{-1})	r^2
		u	v			
Unadjusted	64	-0.012	-0.024	77	2.6	0.94
Slip-adjusted	90	-0.014	-0.033	54	1.8	0.91
Wind-adjusted	74	-0.012	-0.028	69	2.3	0.93
Combined	100	-0.015	-0.037	45	1.4	0.89
Observed	144	-0.013	-0.055			

Figure Captions

FIG. 1. The Southeast U.S. continental shelf (North Carolina (NC), South Carolina (SC), Georgia (GA) and Florida (FL) and the model domain used in this study. The finite element mesh contains 9606 nodes and 18,691 elements. The location of the SABSOON R6 and R2 Towers are shown with triangles. Gray's Reef National Marine Sanctuary (GRNMS) is shown with a square and the Ft. Pulaski and St. Augustine NOS water level stations are shown with diamonds. The 15-, 25-, 50-, 75-, 100-, 500- and 1000-m isobaths are shown.

FIG. 2. a) The u (east-west) wind stress at GRNMS. b) The same for v (north-south). Note the scale difference from a). c) Model drifter velocity adjustment for drifter slippage and wind stress difference in the u (east-west) direction. d) Model drifter velocity adjustment for drifter slippage and wind stress difference in the v (north-south) direction.

FIG. 3. a) The u (east-west) and v (north-south) low-pass filtered drifter velocities for the 3 observed drifters. Also included are the mean u and v velocities for the period shown. b) The same for the fully adjusted model plus the rms error between the observed and numerical drifters.

FIG. 4. The track of observed drifter 30351 (\diamond - OBS) is compared to the model drifters using the unadjusted drogue code (x - MO), the slip-adjusted drogue code (\circ - MS), the wind-adjusted drogue code ($*$ - MW) and the wind-slip adjusted code (\triangle - MWS) at each daily location. A large square and a label (OBS, MO, MS, MW, MWS) annotate the end of the track. The 5-, 10-, 15-, 20-, and 25-m isobaths are shown.

FIG. 5. Distance between model and observed drifters from release. The unadjusted model = x , the slip model = \circ , the wind model = $*$ and the wind-slip model = \triangle . The slopes of the linear regressions are shown.

Figures

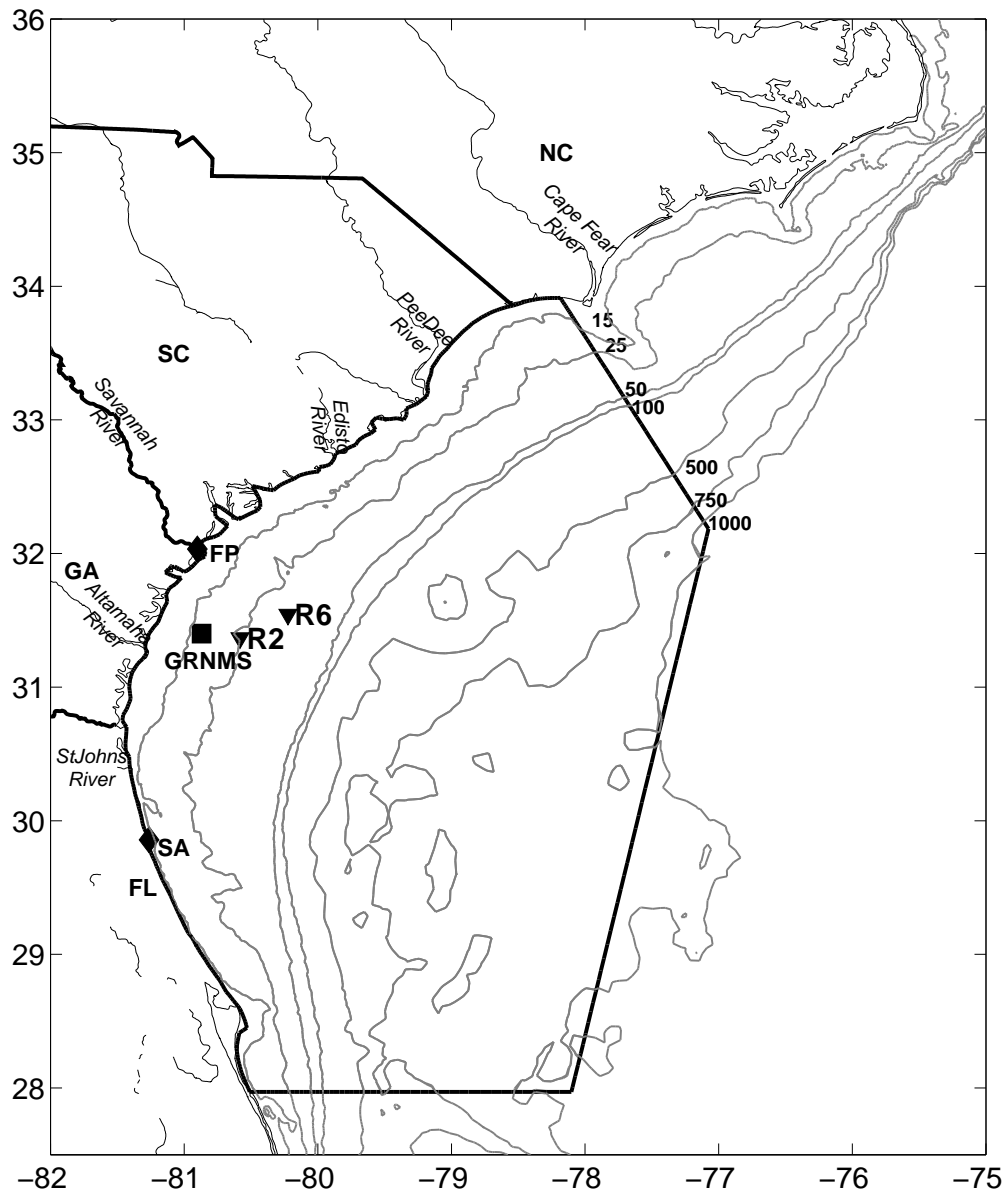


FIG. 1. The Southeast U.S. continental shelf (North Carolina (NC), South Carolina (SC), Georgia (GA) and Florida (FL) and the model domain used in this study. The finite element mesh contains 9606 nodes and 18,691 elements. The location of the SABS00N R6 and R2 Towers are shown with triangles. Gray's Reef National Marine Sanctuary (GRNMS) is shown with a square and the Ft. Pulaski and St. Augustine NOS water level stations are shown with diamonds. The 15-, 25-, 50-, 75-, 100-, 500- and 1000-m isobaths are shown.

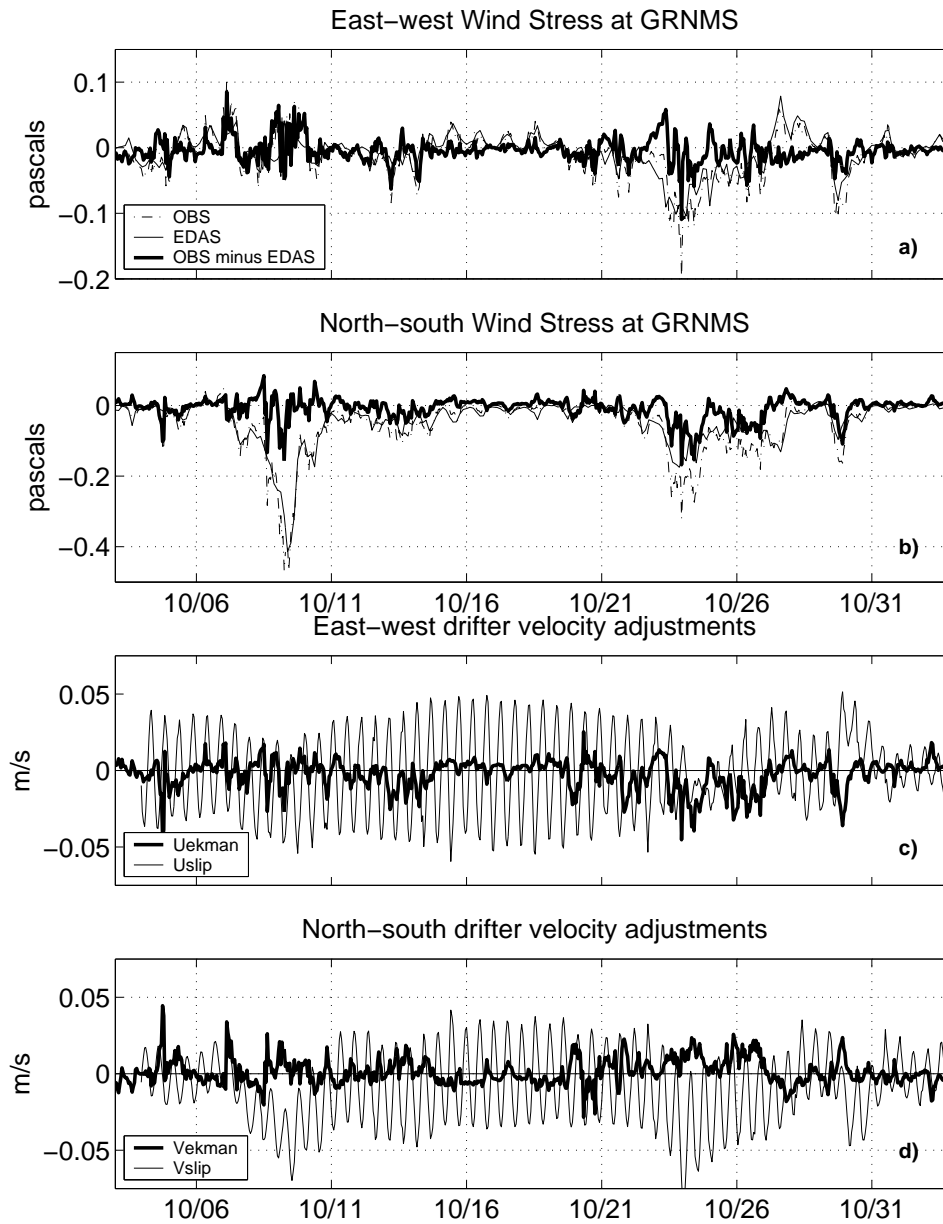


FIG. 2. a) The u (east-west) wind stress at GRNMS. b) The same for v (north-south). Note the scale difference from a). c) Model drifter velocity adjustment for drifter slippage and wind stress difference in the u (east-west) direction. d) Model drifter velocity adjustment for drifter slippage and wind stress difference in the v (north-south) direction.

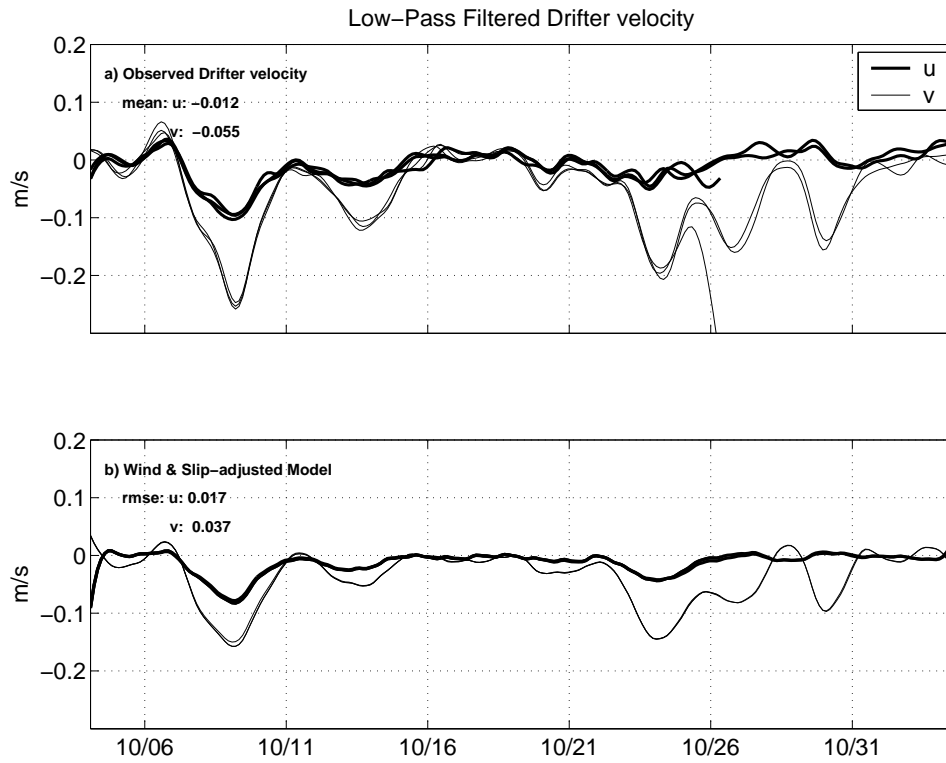


FIG. 3. a) The u (east-west) and v (north-south) low-pass filtered drifter velocities for the 3 observed drifters. Also included are the mean u and v velocities for the period shown. b) The same for the fully adjusted model plus the rms error between the observed and numerical drifters.

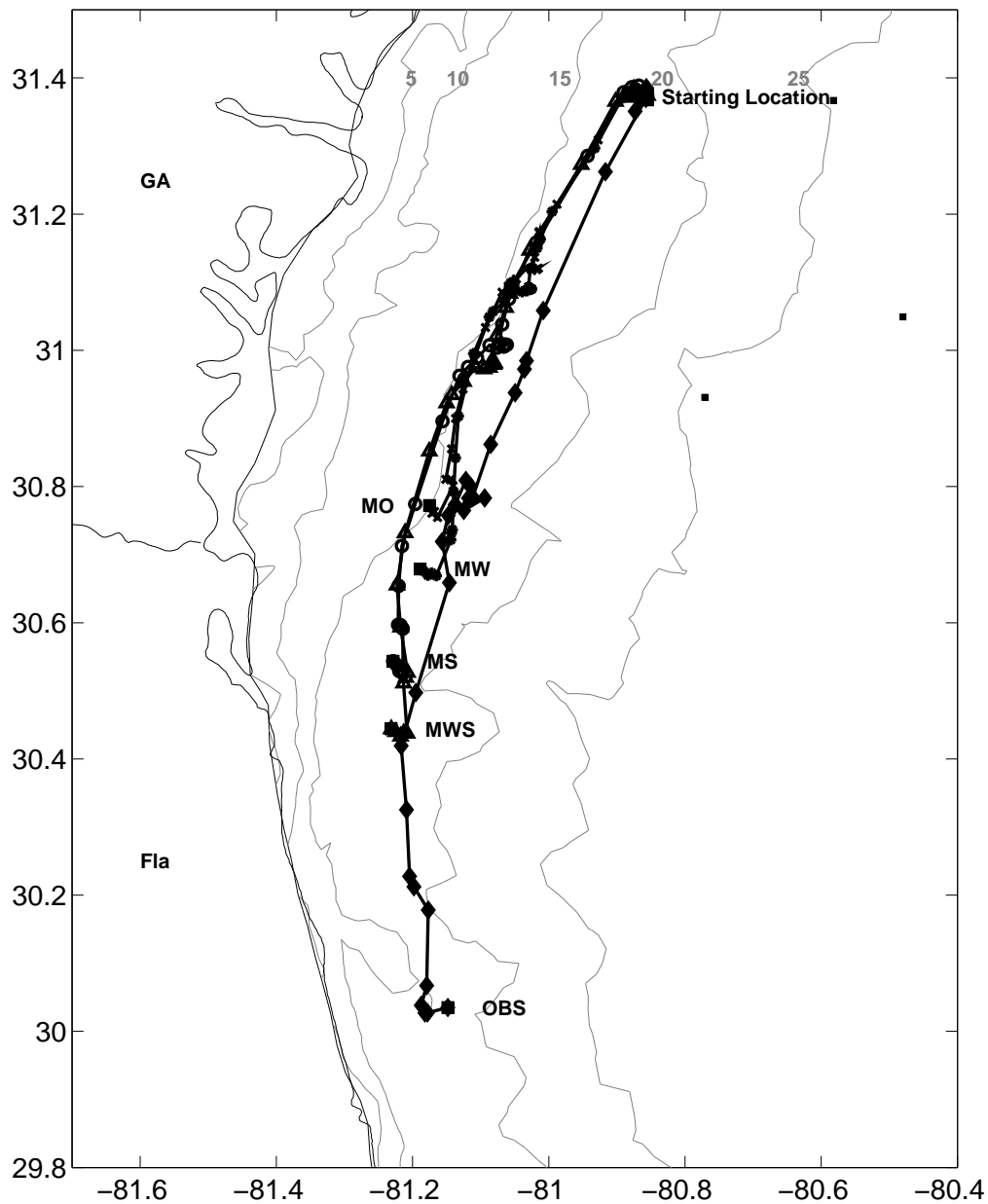


FIG. 4. The track of observed drifter 30351 (\diamond - OBS) is compared to the model drifters using the unadjusted drogue code (x - MO), the slip-adjusted drogue code (\circ - MS), the wind-adjusted drogue code (* - MW) and the wind-slip adjusted code (\triangle - MWS) at each daily location. A large square and a label (OBS, MO, MS, MW, MWS) annotate the end of the track. The 5-, 10-, 15-, 20-, and 25-m isobaths are shown.

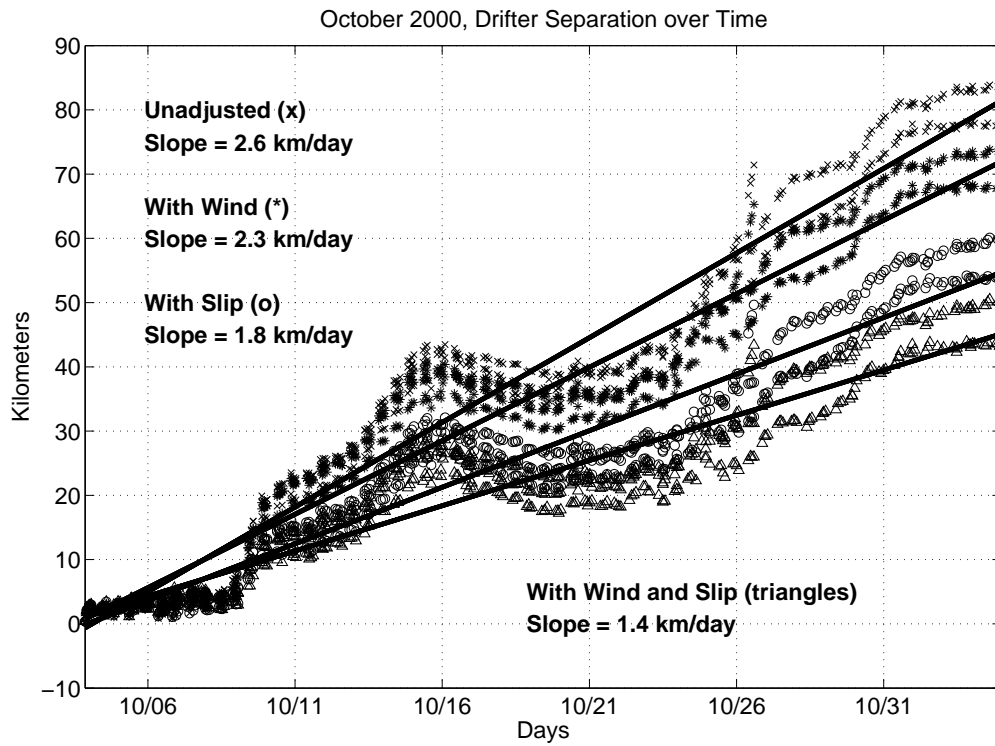


FIG. 5. Distance between model and observed drifters from release. The unadjusted model = x, the slip model = o, the wind model = * and the wind-slip model = Δ . The slopes of the linear regressions are shown.